Energy and Power 2020, 10(1): 1-10
DOI: 10.5923/j.ep.20201001.01

Comparative Numerical Study of the Combustion of a Biofuel Model and Gasoline under Fluent Code

Kamdem K. Claude Aurélien[1,*], Zhu Xiaolu[1,2,3], Harouna K. Attaher[1], Holman Joseph B.[1], Alaeldin Mohamed Tairab[1]

[1]College of Mechanical & Electrical Engineering, Hohai University, Changzhou, Jiangsu, China
[2]Changzhou Key Laboratory of Digital Manufacture Technology, Hohai University, Changzhou, Jiangsu, China
[3]Jiangsu Key Laboratory of Special Robot Technology, Hohai University, Changzhou, Jiangsu, China

Abstract Nowadays, the possibility of substituting gasoline fuel with biofuels is examined by numerous researchers. This paper discusses the numerical study of the biofuel model (methyl decanoate). The Fluent code was used to validate the comparison between the non-premixed gasoline (n-decane) and biofuel model (methyl decanoate) combustion in the same conditions. The turbulence model used was the realizable k-ε model. The aerothermochemistry equations and the transport model of chemical species (Eddy-dissipation) were implemented in the combustion reaction to develop the velocity, pressure, temperature, energy, enthalpy, the turbulence dissipation rate, the kinetic energy of the turbulence, and the mass fraction of the species. The results showed that the CO_2 and NO_X contents of methyl decanoate are 5.7% and 11.03% respectively higher than those of decane.

Keywords Turbulence, Biofuel, Combustion, Eddy-dissipation, Non-premixed

1. Introduction

Considered as the most used means of transportation, the automobile has been put into the center of an environmental controversy over the last few decades of its fossil fuel source, oil, which power its internal combustion engine [1], [2]. The increasingly stringent requirements of the air pollution standard require the development of engines that meet environmental standards [3]. The transformation of this fossil energy into mechanical energy capable of ensuring the displacement of the automobile is taken by the combustion of this hydrocarbon whose resources are limited. Moreover, this combustion results in the formation of pollutants for the environment (destruction of the ozone layer by nitrogen oxides and global warming by carbon dioxide) [4]. Confronted with this threat to the environment, industrials transport sectors are trying to find ways to limit the consumption of fossil fuels and the impact of products from their combustion on the environment. These objectives, which represent major challenges for renewable energy sources, require research on fundamental and technological aspects. To meet the various constraints in terms of the availability of fossil energy resources and to contribute to the reduction of greenhouse gas emissions, multiple solutions are envisaged: one of these solutions arises from the use of biofuels.

Biofuel is identified as a liquid or gaseous fuel obtained from biomass. Biofuels are classified under three categories: first-generation biofuels made from vegetable oils of edible sugar and starch [5], second-generation biofuels based on the non-edible vegetable matter [6], third-generation biofuels made from algae and other micro-organisms [7]. The last category of biofuel offers a more promising alternative than the two previous ones, that pose problems related to the cultivable surfaces and especially of famine due to the rise in prices of some staple foods, such as maize, soy, wheat, rapeseed, sunflower, and palm. Indeed, biofuels are separated into alcohol which is primarily used in the spark-ignition engine "gasoline engine", and esters which are employed in compression ignition engines "diesel engine" [8], [9]. Bioethanol is obtained from vegetable raw materials. Nowadays, it is the most utilized biofuel in the world. It is produced in three different ways from biomass: by fermentation [10], gasification followed by a synthesis process [11], and hydrolysis followed by a fermentation process [12]. Biodiesel is a vegetable oil ester. The use of vegetable oil as fuel is not a new technique. However, these oils offer overly high viscosity and a cetane index (ability to auto-ignition) overly low compared to diesel fuel, that makes them problematic for direct use in a conventional

* Corresponding author:
kamdemclaude@hhu.edu.cn (Kamdem K. Claude Aurélien)
Published online at http://journal.sapub.org/ep

diesel engine, but due to their higher density, the weak power calorific value of vegetable oils is compensated (less than 11.5% gasoline standards) [13]. Therefore, their low cetane index of oils can increase fuel consumption, engine noise and emissions in *HC*, NO_X, and CO_2 [14], [15]. The CO_2 emitted during the combustion from biofuels is taken up by the tree end of plants during growth and presented some advantages and limitations in atmospheric air [16]. To obtain characteristics similar to petroleum diesel, these vegetable oils will undergo transesterification with alcohol, mainly methanol (note that ethanol could be utilized) [17]. This reaction is achieved using a basic or acidic catalyst at moderate temperature (20 - 80 ℃) and atmospheric pressure.

This paper chooses a representative combustion chamber as the basic element for combustion reaction, and simulates the pressure, temperature, velocity and species distribution derived from the combustion. The interaction between the turbulence (model of turbulence and transport model of chemical species) and the combustion has been also examined. These obtained results demonstrate that the biofuel model (methyl decanoate $\boldsymbol{C_{11}H_{22}O_2}$) generates the content of CO_2 and NO_X higher than those of gasoline (n-decane $\boldsymbol{C_{10}H_{22}}$). This study also promotes the comprehension of different physicochemical phenomena issued from the non-premixed combustion of biofuel model in a combustion chamber. The fundamentals variables such as the pressure, temperature, velocity, energy, enthalpy, turbulence dissipation rate, the kinetic energy of turbulence and mass fraction of species are also validated by comparing the results obtained from the simulation of gasoline in the same conditions and parameters that have been settled.

2. Materials and Methods

2.1. Governing Equations

Combustion modeling integrates the flow of fluids based on the equations of fluid mechanics, the transport of species based on the balance of the transported species, and the heat transfer based on the energy balance.

2.1.1. Equations of Aerothermochemistry

The starting point for the turbulent reactive flow analysis is the fluid mechanics equation called the "Navier – Stoke's equation" plus the energy equation. The chemical reactions produced during the flow require that the mass balance of the species present in the reaction and the diffusion phenomena be taken into account. These five equations are as follows [18]:

- Equation of continuity:

$$\frac{\partial \rho}{\partial t} + \frac{\partial (\rho u_j)}{\partial x_j} = 0 \tag{1}$$

- Conservation equation of momentum:

$$\frac{\partial}{\partial t}(\rho u_i) + \frac{\partial}{\partial xi}(\rho u_i u_j) = -\frac{\partial p}{\partial x_i} + \frac{\partial \tau_{ij}}{\partial x_j} \tag{2}$$

(I, j = 1, 2, 3), With the Reynolds stress tensor [19]: $\tau_{ij} = -\mu_t(\frac{\partial u_i}{\partial x_j} + \frac{\partial u_j}{\partial x_i}) + \frac{2}{3}\frac{\partial u_i}{\partial u_j}\mu_t \delta_{ij}$, μ_t the turbulent viscosity, and δ_{ij} the Kronecker symbol.

- Balance equation of the species *k*:

$$\frac{\partial}{\partial t}(\rho Y_k) + \frac{\partial}{\partial x_i}(\rho u_j Y_k) = -\frac{j_j^k}{\partial x_j} \rho \dot{w}_k \tag{3}$$

with (k= 1, n). Where the chemical reaction rate is: $\dot{w}_k = \rho \cdot \Omega_k$, Y_k the mass fraction, and j_j^k is the diffusion flux of the species *k* given by Fick's law [20]: $j_j^k = -\rho D_{kj}\frac{\partial Y_k}{\partial x_j}$, where D_{kj} the molecular diffusivity of the species *k.*

- Energy conservation equation:

$$\frac{\partial}{\partial t}(\rho h_T) + \frac{\partial}{\partial x_j}(\rho u_j h_T) = \frac{\partial p}{\partial t} + \frac{\rho}{\partial x_j}(j_j^h + u_i \tau_{ij}) \tag{4}$$

With the total enthalpy $h_T = h + \frac{1}{2}u_k^2$,

and the diffusion flux of the enthalpy given by the Fourier law [21]: $j_j^h = \frac{\lambda}{c_p}\frac{\partial h}{\partial x_j}$

- State equation of perfect gases:

$$P = \rho \frac{R}{M} T \tag{5}$$

With *M* the molar mass (g/mol), *R* the constant of perfect gases, *T* the reference temperature (K), and ρ the density.

2.1.2. Chemistry Kinetic

All the chemical reactions involved can be written in the following general form [22]:

$$\sum_{k=1}^{k} \nu_k^{'} Y_k \rightleftharpoons \sum_{k=1}^{k} \nu_k^{"} Y_k \tag{6}$$

Where $\nu_k^{'}$ and $\nu_k^{"}$ are respectively the stoichiometric coefficients in the forward and reverse direction, Y_k is a chemical species of the considered gas.

2.1.2.1. Chemical Production Rate

If species k is involved in several chemical reactions, its global production rate $\dot{w}_k$ is written:

$$\dot{w}_k = M_k \sum_{k=1} (\nu_{ki}^{"} + \nu_{ki}^{'}) q_i \tag{7}$$

q_i is the difference between the direct and inverse volume velocity of the reaction i. It is given by:

$$q_i = k_{fi}\prod_{k=1}^{k}[x_k]^{\nu'_{ki}} - K_{ri}\prod_{k=1}^{k}[x_k]^{\nu''_{ki}} \quad (8)$$

With $x_k = \frac{\rho Y_k}{M_k}$

2.1.2.2. Reaction Velocity

It has been shown experimentally that reaction rates depend on temperature and generally follow an Arrhenius type law [23]:

$$k_{fi} = A_{fi}T^{Bfi}\exp(-\frac{E_{fi}}{RT}); k_{ri} = A_{ri}T^{Bri}\exp(-\frac{E_{ri}}{RT}) \quad (9)$$

Where $A_{fi}, B_{fi}, A_{ri}, B_{ri}, E_{ri}$ are dependent on the considered reaction.

2.2. Problem Description and Boundary Conditions

The agitated combustion cylinder is shown in Figure 1. It is 1.8 m long and 0.45 m in diameter. At the center of the cylinder, a 0.01 m interior diameter tube is provided for the biofuel inlet.

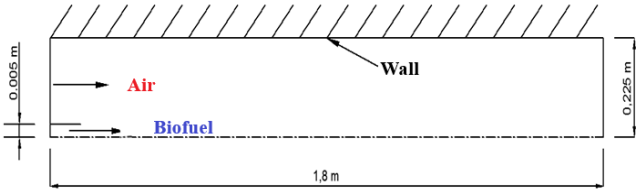

Figure 1. Combustion chamber

The boundary conditions set for this simulation are presented in Table 1:

Table 1. Boundary conditions

Type of conditions	entities	Temperature (K)	Velocity (m / s)	Pressure (bars)
Inlet	Air	300	1100 [24]	/
	Biofuel	300	200 [5]	50 [24]
Outlet	Outlet	/	/	Atmospheric Pressure
Wall	Wall	300	V=0	/

2.3. Numerical Method

The method used by the FLUENT code is that of the finished volumes [25]. It stands out for its reliability in results, its adaptation to physical problems, its ability to cope with complex geometries. Besides, it is characterized by its advantage to satisfy the conservation of mass, momentum, and energy in all the finished volumes as well as in the whole field of computation, which is not the case with the other methods. It facilitates the linearization of nonlinear terms in conservation equations.

It should be noted that Fluent offers several models for the modeling of reactive flows, but the model of the species chosen for this simulation is the transport model of chemical species and the volumetric reaction to "Eddy-Dissipation" as the interaction between turbulence and chemistry.

This choice is motivated by [26]. In this case, the combustion, which is only controlled by turbulence, transports the mixture of the fresh gases with the hot products in the reaction zone, where the chemical kinetics are rapidly carried out.

The Fluent software also provides several turbulence models such as Spalmart-Allmaras, $k-\varepsilon$ models, $k-\omega$ Models, Reynolds stress model (RSM), Detached eddy simulation (DES) model, Large-eddy simulation (LES) model [27]. In this study, the standard model k-ε was utilized. It is used as a model with two transport equations, one for the kinetic energy of the turbulence k and one for the rate of dissipation of the kinetic energy ε. This model presents some advantages such as it assumes that the turbulent regime is fully established throughout the domain and that the effects of molecular viscosity are negligible compared to those of the turbulent viscosity (far from the walls). It is based on the Boussinesq hypothesis, that there is an analogy between the action of viscous forces and the Reynolds constraints in the mean flow [28]:

$$\bar{\rho}\tilde{u_i''}u_j'' = \frac{2}{3}\bar{\rho}\delta_{ij}(k + \frac{\mu_t}{\bar{\rho}}\frac{\partial\tilde{u_k}}{\partial x_k}) - \frac{\mu_t}{\bar{\rho}}(\frac{\partial\tilde{u_i}}{\partial x_j} + \frac{\partial\tilde{u_j}}{\partial x_i}) \quad (10)$$

The model calculates the turbulent viscosity μ_t by using the kinetic energy of turbulence k and the rate of dissipation of the kinetic energy of turbulence ε as follows:

$$\mu_t = \rho C_\mu \frac{k^2}{\varepsilon}$$

The transport equations are written as follows:

- Equation of the turbulence kinetic energy:

$$\frac{\partial\bar{\rho}k}{\partial t} + \frac{\partial\bar{\rho}k\tilde{u_j}}{\partial x_j} = \frac{\partial}{\partial x_j}(\frac{\mu_t}{\sigma_k}\frac{\partial k}{\partial x_j}) + \bar{\rho}\tilde{u_i''}u_j''\frac{\partial u_i}{\partial x_j} - \bar{\rho}\varepsilon \quad (11)$$

- Equation of the dissipation rate of kinetic energy

$$\frac{\partial\bar{\rho}\varepsilon}{\partial t} + \frac{\partial\bar{\rho}\varepsilon\tilde{u_j}}{\partial x_j} = \frac{\partial}{\partial x_j}(\frac{\mu_t}{\sigma_k}\frac{\partial\varepsilon}{\partial x_j}) + c_{\varepsilon 1}\frac{\varepsilon}{k}\bar{\rho}\tilde{u_i''}u_j''\frac{\partial u_i}{\partial x_j} - c_{\varepsilon 2}\bar{\rho}\frac{\varepsilon^2}{k} \quad (12)$$

These equations involve empirical coefficients $C_\mu, \sigma_k, \sigma_\varepsilon, C_{\varepsilon 1}, C_{\varepsilon 2}$ listed in Table 2, on that the calculation results depend.

Table 2. Empirical values of the Standard model k-ε model [27]

C_μ	σ_k	σ_ε	$C_{\varepsilon 1}$	$C_{\varepsilon 2}$
0.09	1.00	1.30	1.44	1.92

2.3.1. Mesh

The mesh is obtained automatically after selecting the parameters. The mesh element chosen is quadrilateral of Map type. For this mesh, it is obtained a result of 5000 nodes that can be seen in Figure 2. The size of the meshes differs from one point to another of the geometry.

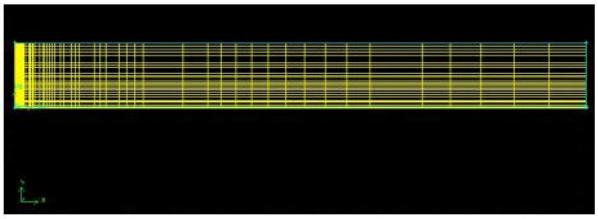

Figure 2. Generation of the mesh of the combustion chamber in GAMBIT

2.3.2. Simulation Parameters

According to their investigation [15], the values of some properties of biofuels model developed in kinetic models are found in Table 3.

Table 3. Some examples of model fuels developed in kinetic models

Fuel real	Fuel model	Mass volume (g / Ml) to 293 K	Index of cetane	Family chemical
Biodiesel	Octanoate methyl	0.890 [15]	33.6 [15]	Ester
	Decanoate methyl	0.871 [29]	47.7 [29]	

The physicochemical characteristics and properties of the gasoline and biofuel model used for this work are shown in Table 4:

Table 4. Physicochemical characteristics of the fuels and biofuels used

	Gasoline	Biofuel model
Chemical formula	n-decane $C_{10}H_{22}$	Decanoate methyl $C_{11}H_{22}O_2$
Molar mass (g / mol)	142	186
Density (kg / m^3)	7.3 [30]	8.8 [31]
Kinematic viscosity (m^2 / s)	1.26 10^{-6} [30]	5.617395 10^{-6}[31]
Thermal conductivity (w / m.k)	0.15 [30]	0.153 [31]
Standard enthalpy (j / mol)	-640 500 [32]	-300 900[32]
Specific heat (j / kg.k)	2000 [30]	2070 [33]
Reference temperature (k)	298.15 [27]	373 [33]
Index of cetane	55 [15]	47 [31]

2.3.3. Combustion Reaction

Pure components were chosen to analyse the biofuel and gasoline. The combustion reaction is defined in terms of the stoichiometric coefficients, formation enthalpy and control parameters of the reaction rate. In this study, it is a one-step reaction scheme with five (06) species $C_{10}H_{22}$ *or* $C_{11}H_{22}O_2$, CO_2, H_2O, O_2, N_2 (inert), and NOx was chosen.

- The oxidation of n-decane of chemical formula $C_{10}H_{22}$ for the gasoline.

According to the general hydrocarbon combustion equation of n-decane, it can be written this following equation:

$$C_{10}H_{22} + 15.5(O_2 + 3.78N_2) \rightarrow 10CO_2 + 11H_2O + 58.59N_2 \quad (13)$$

The stoichiometric ratio ϕ_s associated for this reaction is

$$\phi_s = \frac{n_a}{n_c} = \frac{15.5(32 + 3.78 \times 28.16)}{12.011 \times 10 + 1.008 \times 22} = 15.08$$

Therefore, complete combustion of a unit of gasoline mass requires 15.08 units of an air mass.

- Determination of the Reynolds number of $C_{10}H_{22}$

$$\mathrm{Re}_{C_{10}H_{22}} = \frac{v \cdot d}{\nu} = \frac{200 \times 0.01}{1.26 \times 10^{-6}} = 1587301.58$$

- The oxidation of methyl decanoate of chemical formula $C_{11}H_{22}O_2$ for the biofuel

Methyl decanoate belongs to the family of esters given its chemical formula. The general equation of combustion of the esters is given by [30]:

$$C_nH_{2n}O_2 + \frac{(3n-2)}{2}(O_2 + 3.78N_2) \rightarrow nCO_2 + nH_2O + 3.78\frac{(3n-2)}{2}N_2 \quad (14)$$

This relation allows to write the following equation:

$$C_{11}H_{22}O_2 + 15.5(O_2 + 3.78N_2) \rightarrow 11CO_2 + 11H_2O + 58.59N_2 \quad (15)$$

The stoichiometric ratio ϕ_s associated for this reaction is:

$$\phi_s = \frac{n_a}{n_c} = \frac{15.5(32 + 3.78 \times 28.16)}{12.011 \times 11 + 1.008 \times 22 + 32} = 11.52$$

Thus, complete combustion of a biofuel mass unit requires 11.52 air mass units.

- Determination of the Reynolds number of $C_{11}H_{22}O_2$

$$\mathrm{Re}_{C_{11}H_{22}O_2} = \frac{v \cdot d}{\nu} = \frac{200 \times 0.01}{5.617395 \times 10^{-6}} = 356036.91$$

Based on the obtained values of the stoichiometric ratio of both biofuel, it is deducted that the combustion is lean because the air coefficient lambda is greater than 1. Therefore, theoretically, these values are very significant and prove that there is a high quantity of NOx issued from this combustion due to the high temperature generates by both fuel. In addition, both Reynolds numbers obtained prove that the regime is turbulent.

The formation of NOx is illustrated by the extended Zeldovich mechanism [34]. The fuel provides high heat and due to the presence of free nitrogen and excess oxygen in compression combustion. This increases the appearance of NOx which forms under catalysis during combustion. His overall reaction is:

$$O_2 + N_2 \longleftrightarrow 2NO \quad (16)$$

3. Results and Discussions

3.1. Static Pressure

The results of this study presented in Figure 3 show a very high pressure at the entrance to the combustion chamber. As this combustion takes place, this pressure drops and is submitted to atmospheric pressure at the outlet. Moreover, it is noted in this Figure 3 that the pressure of methyl decanoate (1,2555x10^7 Pa) remains slightly higher than the pressure of decane (1,28476x10^7 Pa). This high pressure is due to the extreme heat released during the premix combustion, such as indicates [35]. This gradually relaxes as the premix flame gives way to the diffusion flame. Both pressure drop and end up at the atmospheric pressure at the outlet. This pressure relief is indicated on the domain by the gradual coloration in blue towards the outlet of the chamber. In view of this point, the model biofuel also generates a remarkable pressure and is significant compared to gasoline.

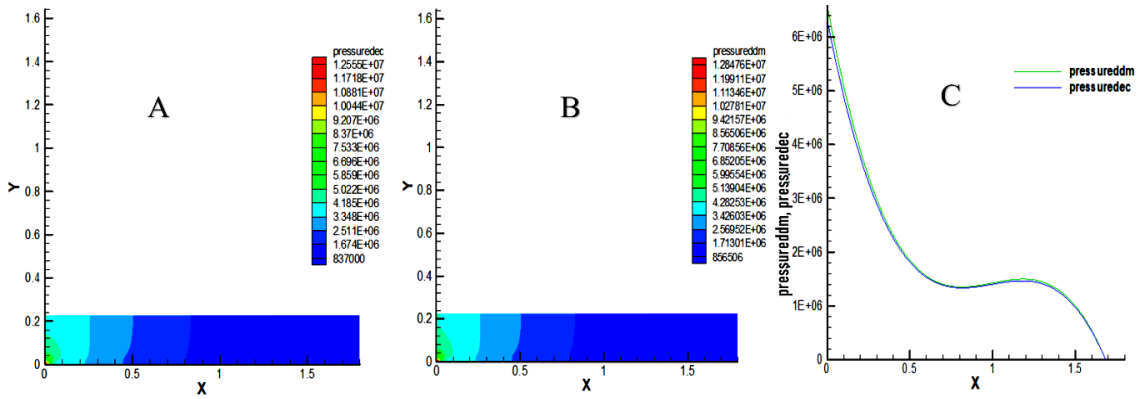

Figure 3. Static pressure in the combustion chamber. (A) pressure of decane (dec), (B) Pressure of methyl decanoate (ddm), (C) comparison between pressure of decane and pressure of methyl decanoate

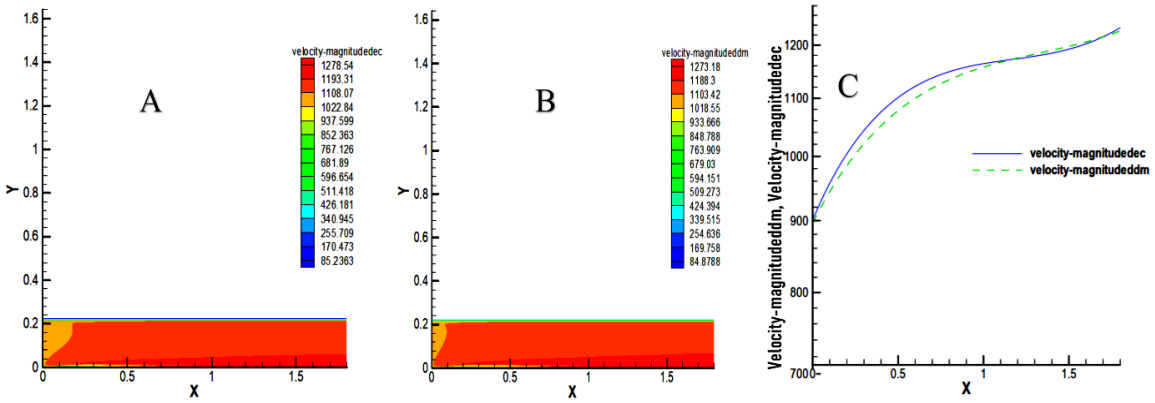

Figure 4. Velocity distribution in the combustion chamber. (A) velocity of decane (dec), (B) velocity of methyl decanoate (ddm), (C) comparison between velocity of decane and Velocity of methyl decanoate

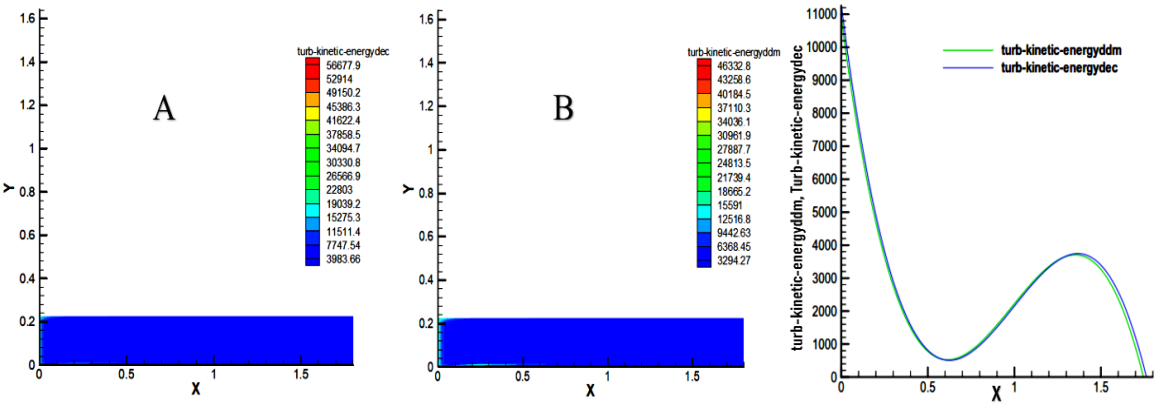

Figure 5. Turbulence kinetic energy distribution in the combustion chamber. (A) Turbulence kinetic energy of decane (dec), (B) Turbulence kinetic energy of methyl decanoate (ddm), (C) comparison between Turbulence kinetic energy of decane and Turbulence

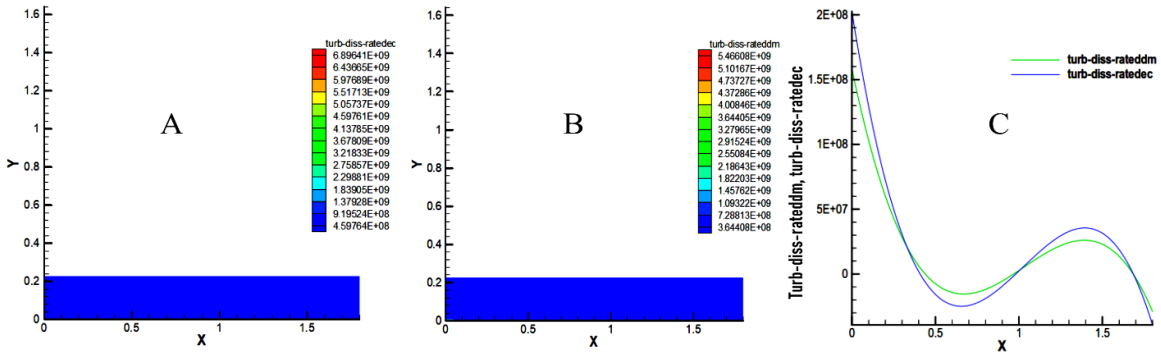

Figure 6. Turbulence dissipation rate distribution in the combustion chamber. (A) Turbulence dissipation rate of decane (dec), (B) Turbulence dissipation rate of methyl decanoate (ddm), (C) comparison between Turbulence dissipation rate of decane and Turbulence dissipation rate of methyl decanoate

3.2. Velocity Distribution

The velocity distribution indicates by their dark red coloring a maximum speed on the axis of symmetry of the chamber as indicated in Figure 4. There are maximum velocities substantially equal to the outlet of the chamber, supposedly 1278.54 m / s for decane and 1273.54 m / s for methyl decanoate. In the near wall, relatively low speeds of about 340.945 m / s and 339.315 m / s respectively are observed for decane and methyl decanoate.

Based on the Figure 4, the decane velocity is higher than the biofuel velocity in the range of 0 to 1.2 m. At this point on the X axis of the combustion chamber where they intersect at a velocity of about 1175 m / s, the decanoate velocity is above that of decane up to 1.6 m.

3.3. Kinetic Energy of Turbulence

The results show a very high turbulence at the inlet of the chamber, which is of the order of 56677.6 m^2 / s^2 for decane and 46332.8 m^2 / s^2 for the methyl decanoate as indicated in Figure 5. This high kinetic energy has a relationship with the high pressure at the entrance of the chamber for both fuels. It decreases sharply to 0.6 m. In the zone [0 - 0.6] m, the kinetic energy of decane is slightly higher than that of decanoate. In the zone [0.6 - 1.3] m, that of decanoate is slightly higher. Finally, in the zone [1.3 - 1.8] m, the kinetic energy of the decane is slightly higher than that of the biofuel with an pproximate percentage of 18.25%.

3.4. Turbulence Dissipation Rate

In this study, we note on the dissipation rate fields a high rate at the entrance of the combustion chamber. With values of 6.89641x109 m^2 / s^3 for decane and 5.46608x109 m^2 / s^3 for methyl decanoate as shown in Figure 6.

A high turbulence dissipation rate is observed at the inlet, with a higher decane turbulence dissipation rate. The two curves intersect at points x = 0.35 m, x = 1.02 m and x = 1.7 m. Then, there is zero variation at the output for the decane. At the point x = 0.65 m, the turbulence dissipation rate of methyl decanoate is higher than that of decane, and at the point x = 1.4 m it is observed a dissipation rate of decane higher than that of decanoate. The dissipation rate of methyl decanoate is 20.7% lower than dissipation rate of decane.

3.5. Temperature Distribution

The results of this study show a very high temperature in the axis of the combustion chamber that is due to the inflammation of the mixture. Decane reaches a maximum temperature of 2615.77K, and methyl decanoate has a maximum temperature of 2645.68K as showed in Figure 7. Moreover, this temperature will recover more and more in nearby wall to allow the engine to operate under normal conditions. In the zone [0 - 1.03] m, the temperature of the decane is higher than that of the decanoate, then the trend is reversed in the zone [1.3 - 1.8] m. The temperature generates by the methyl decanoate is 1.13% higher than the temperature of decane. Therefore, the low cetane index of biofuels generates a rise in temperatures [15].

3.6. Total Energy

The results indicate a very high total energy due to the high intensity of heat produced during combustion of the mixture in the combustion chamber. Inflammation of the air-fuel mixture allows to generate the maximum energies of 556983 J / kg for decane and 553604 J / kg for decanoate of methyl as showed in Figure 8.

It is noted a decrease in the zone [0 - 0.4] m, then a rapid growth until the outlet for both fuels. The total energy of the decane being always greater than the energy of the decanoate of methyl. The energy of both fuel has the same profile, but the energy produces in the methyl decanoate is 0.6% lower than the energy of decane. The study of the application of energy and exergy analyses to an IC engine using biodiesel fuel showed that the energy generates by biofuels is 8.2% lower than diesel fuel [36]. This result shows that this value is significant and proves that the methyl decanoate can be employed in the same conditions as the decane.

3.7. Total Enthalpy

It is observed that these two fuels emit a very high enthalpy following the ignition of the mixture in the axis of the combustion chamber to the outlet. Maximum values reached are 1.06386x106 J / kg for decane and 1.03805x106 J / kg for methyl decanoate as indicated in Figure 9. These

curves show that the total enthalpy of decane is greater than the enthalpy of methyl decanoate in the combustion chamber with an approximate percentage of 2.38%.

3.8. The Mass Fraction of CO_2

In this study, the results show that the content biofuel of CO_2 is 0.176432 compared to gasoline which is 0.166239. This value of biofuel is high and presents an increase of approximatively 5.7% relative to decane as indicated in Figure 10.

The curve of methyl decanoate is still above of the decane curve. That means biofuels produce a lot of CO_2 which is very important. Therefore, the effect of coconuts biodiesel blended fuel on engine performance and emission characteristics has been studied and it was found that the engines exhaust gas emissions generate the high CO_2 for biodiesel blended fuel compares to diesel fuel [14]. Thus, this can be explained by their low cetane index of biofuels that can increase the content of CO_2 [15]. Therefore, the value obtained from this simulation is remarkable.

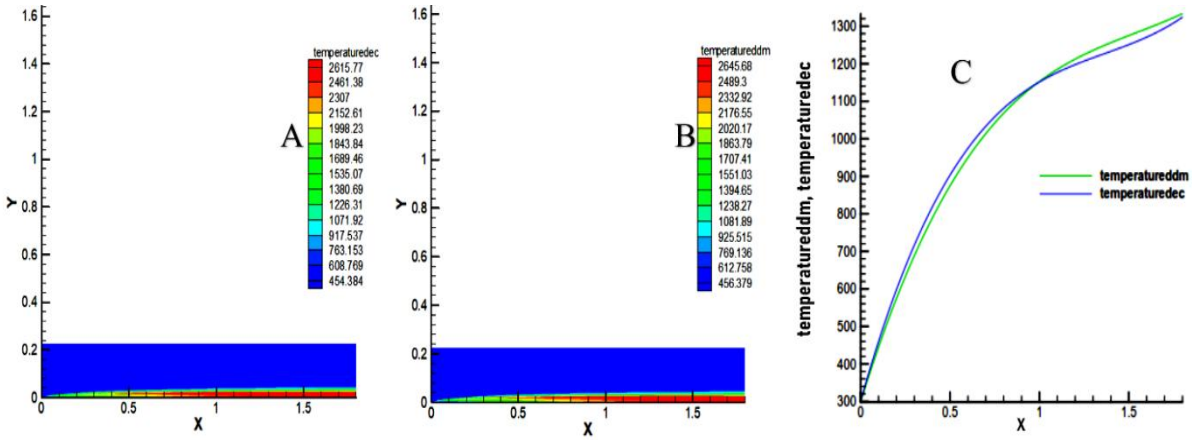

Figure 7. Temperature distribution in the combustion chamber. (A) Temperature of decane (dec), (B) Temperature of methyl decanoate (ddm), (C) comparison between Temperature of decane and Temperature of methyl decanoate

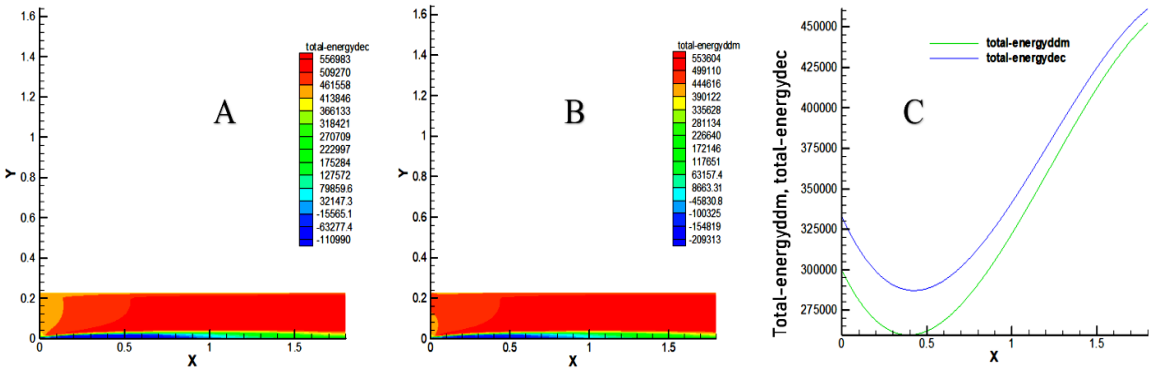

Figure 8. Total energy in the combustion chamber. (A) Total energy of decane (dec), (B) Total energy of methyl decanoate (ddm), (C) comparison between Total energy of decane and Total energy of methyl decanoate

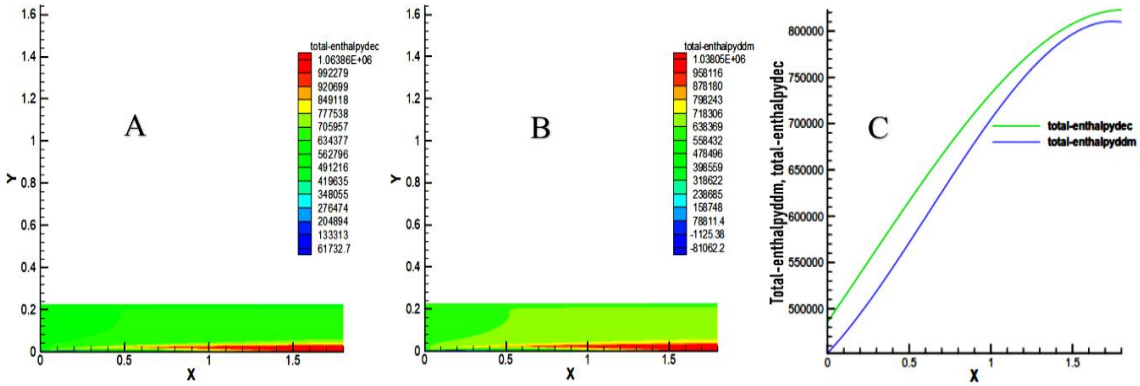

Figure 9. Total enthalpy in the combustion chamber. (A) Total enthalpy of decane (dec), (B) Total enthalpy of methyl decanoate (ddm), (C) comparison be-tween Total enthalpy of decane and Total enthalpy of methyl decanoate

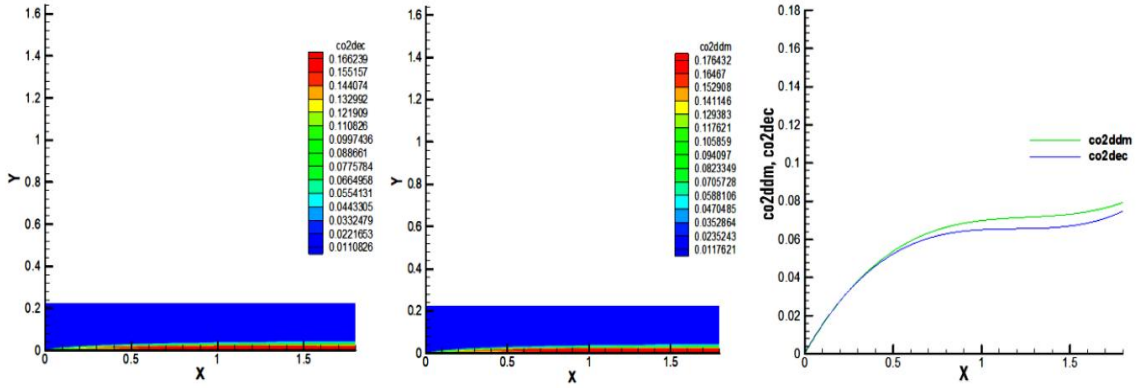

Figure 10. CO_2 mass fraction in the combustion chamber. (A) CO_2 mass fraction of decane (dec), (B) CO_2 mass fraction of methyl decanoate (ddm), (C) comparison between CO_2 mass fraction of decane and CO_2 mass fraction of methyl decanoate

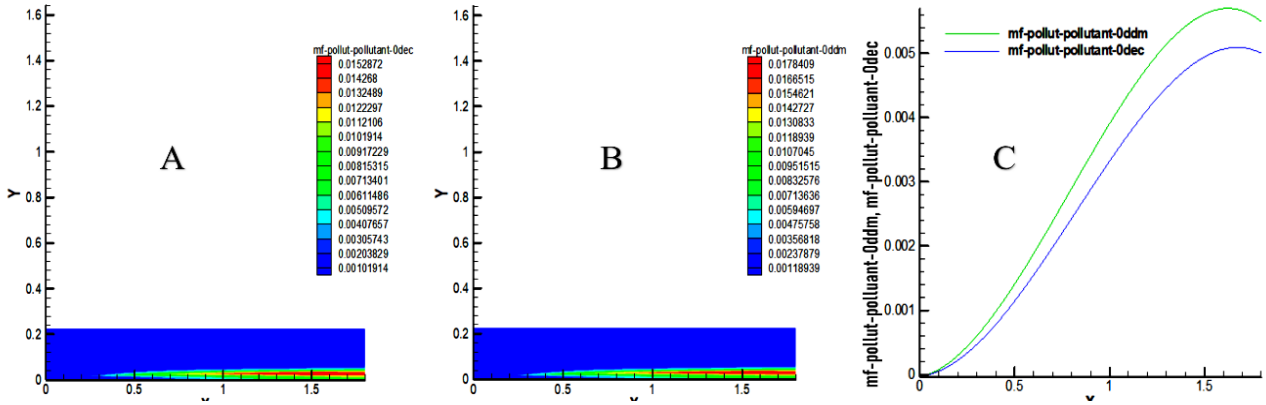

Figure 11. NOx mass fraction in the combustion chamber. (A) NOx mass fraction of decane (dec), (B) NOx mass fraction for methyl decanoate (ddm), (C) comparison between NOx mass fraction of decane and NOx mass fraction of methyl decanoate

3.9. The Mass Fraction of NOx

The results of this study show a NOx mass fraction of 0.015872 for decane and 0.0178409 for methyl decanoate at the outlet of the chamber, an increase of approximately 11.03% relative to decane as indicated in Figure 11. The low cetane index of biofuels generates a rise in NOx levels as well as high temperatures [15]. Thus, NOx emissions for biodiesel blended have been found higher than diesel fuel [14]. Based on this Figure 11, It is noted that the NOx production curve of methyl decanoate is above that of decane, which reflects a high production of NOx by the model biofuel. Consequently, this result is remarkable.

4. Conclusions

The Fluent code is allowed to simulate the combustion of a biofuel model (methyl decanoate $C_{11}H_{22}O_2$) and gasoline (n-decane $C_{10}H_{22}$) under the same conditions. For this simulation, the type of mesh used was quadrilateral of map and it has been obtained 5000 nodes compared to other types. The equations of aerothermochemistry, a turbulence model (the standard k-ε model), the transport model of chemical species (Eddy-dissipation), and the fuel oxidation reaction equations have been implemented. The simulation parameters have been defined based on the literature and the calculation. The results obtained from this simulation show that the NOx content generates in the biofuel is slightly higher 11.03% than the diesel fuel. The maximum energies of 684314 J / kg and 679880 J / kg respectively are found for methyl decanoate and decane. The energy produces in the methyl decanoate is 0.6% lower than the energy of decane. The content of CO_2 produces in the methyl decanoate is 5.7% relative higher than decane. This simulation shows that this biofuel generates an energy comparable to that of diesel fuel, but it releases more pollutants.

ACKNOWLEDGEMENTS

This research was funded by Fundamental Research Funds for the Central Universities of China (grant number 2018B22414), Changzhou Sci &Tech Program (grant number CE20195037) and Youth talent support project from Jiangsu association for science and technology.

Nomenclature

u_i , u_j velocity in direction i, j

ρ density kg/m^3

t time

$\frac{\partial}{\partial x_j}(\frac{\mu_t}{\sigma_k}\frac{\partial k}{\partial x_j})$, $\frac{\partial}{\partial x_j}(\frac{\mu_t}{\sigma_k}\frac{\partial \varepsilon}{\partial x_j})$ diffusive transport

P or p pressure (Pa)

τ_{ij} Reynolds stress tensor (Pa)

Y_k Fraction of species k

j_j^k diffusion flux of the species k (m/s^2)

$\dot{w}_k$ production rate of the species k

Ω_k chemical reaction coefficient of the species k

h enthalpy

u_k velocity of the particle k

λ excess air coefficient

c_p heat capacity at constant pressure (j/kg.K)

$\frac{\partial \bar{\rho} k}{\partial t}$, $\frac{\partial \bar{\rho} \varepsilon}{\partial t}$ temporal transport

$\frac{\partial \bar{\rho} k \tilde{u}_j}{\partial x_j}$, $\frac{\partial \bar{\rho} \varepsilon \tilde{u}_j}{\partial x_j}$ convective transport

A_{fi} , A_{ri} constant

$\bar{\rho} \overline{u_i'' u_j''} \frac{\partial u_i}{\partial x_j}$,

$c_{\varepsilon 1} \frac{\varepsilon}{k} \bar{\rho} \overline{u_i'' u_j''} \frac{\partial u_i}{\partial x_j}$ production rate

$\bar{\rho} \varepsilon$, $c_{\varepsilon 2} \bar{\rho} \frac{\varepsilon^2}{k}$ dissipation rate

ε dissipation of kinetic energy from turbulence (m^3/s^3)

$\bar{\rho}$ average density

$\tilde{u}_j$ average velocity according to Fabre

k constant of Von Kármán

k_{fi} direct rate of reaction

k_{ri} reverse reaction rate

M_k molar mass of particle k

E_{fi} , E_{ri} activation energy of direct and reverse reactions

B_{fi} , $B_{ri,}$ temperature exponent

REFERENCES

[1] I. Dincer, "Environmental impacts of energy," *Energy policy*, vol. 27, no. 14, pp. 845–854, 1999.

[2] A. M. Omer, "Energy, environment and sustainable development," *Renewable and sustainable energy reviews*, vol. 12, no. 9, pp. 2265–2300, 2008.

[3] I. Hascic, F. P. de Vries, N. Johnstone, and N. Medhi, "Effects of environmental policy on the type of innovation: the case of automotive emissions control technologies," *OECD Journal: Economic Studies*, vol. 2009, no. 1, pp. 49–66, 2008.

[4] S. D. Casler and P. D. Blair, "Economic structure, fuel combustion, and pollution emissions," *Ecological economics*, vol. 22, no. 1, pp. 19–27, 1997.

[5] D. P. Ho, H. H. Ngo, and W. Guo, "A mini review on renewable sources for biofuel," *Bioresource technology*, vol. 169, pp. 742–749, 2014.

[6] S. N. Naik, V. V. Goud, P. K. Rout, and A. K. Dalai, "Production of first and second generation biofuels: a comprehensive review," *Renewable and sustainable energy reviews*, vol. 14, no. 2, pp. 578–597, 2010.

[7] A. Singh, P. S. Nigam, and J. D. Murphy, "Renewable fuels from algae: an answer to debatable land based fuels," *Bioresource technology*, vol. 102, no. 1, pp. 10–16, 2011.

[8] W.-H. Leong, J.-W. Lim, M.-K. Lam, Y. Uemura, and Y.-C. Ho, "Third generation biofuels: A nutritional perspective in enhancing microbial lipid production," *Renewable and sustainable energy reviews*, vol. 91, pp. 950–961, 2018.

[9] M. Krzywonos, K. Tucki, J. Wojdalski, A. Kupczyk, and M. Sikora, "Analysis of Properties of Synthetic Hydrocarbons Produced Using the ETG Method and Selected Conventional Biofuels Made in Poland in the Context of Environmental Effects Achieved," *Rocznik Ochrona Środowiska*, vol. 19, 2017.

[10] M. Boluda-Aguilar and A. López-Gómez, "Production of bioethanol by fermentation of lemon (Citrus limon L.) peel wastes pretreated with steam explosion," *Industrial crops and products*, vol. 41, pp. 188–197, 2013.

[11] L. Wei, L. O. Pordesimo, C. Igathinathane, and W. D. Batchelor, "Process engineering evaluation of ethanol production from wood through bioprocessing and chemical catalysis," *Biomass and bioenergy*, vol. 33, no. 2, pp. 255–266, 2009.

[12] G. Chaudhary, L. K. Singh, and S. Ghosh, "Alkaline pretreatment methods followed by acid hydrolysis of Saccharum spontaneum for bioethanol production," *Bioresource Technology*, vol. 124, pp. 111–118, 2012.

[13] J. S. J. Alonso, C. Romero-Ávila, L. S. J. Hernández, and A.-K. Awf, "Characterising biofuels and selecting the most appropriate burner for their combustion," *Fuel processing technology*, vol. 103, pp. 39–44, 2012.

[14] A. M. Liaquat *et al.*, "Effect of coconut biodiesel blended fuels on engine performance and emission characteristics," *Procedia Engineering*, vol. 56, pp. 583–590, 2013.

[15] P. R. L. HELENA, "Etude expérimentale et modélisation cinétique de l'oxydation, l'auto-inflammation et la combustion de carburants Diesel et bio-Diesel.," PhD Thesis, Citeseer, 2012.

[16] A. Jankowski and A. Sandel, "Exhaust emission reduction problems of internal combustion engines fueled with biofuels," *Journal of KONES Internal Combustion Engines*, vol. 10, no. 3–4, 2003.

[17] Z. Helwani, M. R. Othman, N. Aziz, J. Kim, and W. J. N. Fernando, "Solid heterogeneous catalysts for transesterification of triglycerides with methanol: a review," *Applied Catalysis A: General*, vol. 363, no. 1–2, pp. 1–10, 2009.

[18] T. von Karman, "Fundamental equations in aerothermochemistry," *Selected Combustion problems*, vol. 2, 1956.

[19] Z. Han and R. D. Reitz, "Turbulence modeling of internal

combustion engines using RNG κ-ε models," *Combustion science and technology*, vol. 106, no. 4–6, pp. 267–295, 1995.

[20] R. Becker, M. Braack, and B. Vexler, "Parameter identification for chemical models in combustion problems," *Applied numerical mathematics*, vol. 54, no. 3–4, pp. 519–536, 2005.

[21] J. Warnatz, U. Maas, and R. W. Dibble, *Combustion*, vol. 26. Springer, 1999.

[22] S. M. Sarathy, "Chemical kinetic modeling of biofuel combustion," PhD Thesis, 2010.

[23] A. Messadi *et al.*, "A new equation relating the viscosity Arrhenius temperature and the activation energy for some Newtonian classical solvents," *Journal of Chemistry*, vol. 2015, 2015.

[24] B. Vieux and R. Armao, *Les moteurs diesel: technologie professionnelle générale*. Foucher, 1993.

[25] K. Dumont, J. M. A. Stijnen, J. Vierendeels, F. N. Van De Vosse, and P. R. Verdonck, "Validation of a fluid–structure interaction model of a heart valve using the dynamic mesh method in fluent," *Computer methods in biomechanics and biomedical engineering*, vol. 7, no. 3, pp. 139–146, 2004.

[26] B. F. Magnussen and B. H. Hjertager, "On mathematical modeling of turbulent combustion with special emphasis on soot formation and combustion," in *Symposium (international) on Combustion*, 1977, vol. 16, pp. 719–729.

[27] F. U. Guide, *Fluent 6.3. 26*. 2005.

[28] T. Dutta, K. P. Sinhamahapatra, and S. S. Bandyopdhyay, "Comparison of different turbulence models in predicting the temperature separation in a Ranque–Hilsch vortex tube," *International Journal of Refrigeration*, vol. 33, no. 4, pp. 783–792, 2010.

[29] O. Herbinet, W. J. Pitz, and C. K. Westbrook, "Detailed chemical kinetic oxidation mechanism for a biodiesel surrogate," *Combustion and Flame*, vol. 154, no. 3, pp. 507–528, 2008.

[30] I. Martínez and J. M. Perales, "Mechanical behaviour of liquid bridges in microgravity," *Physics of fluids in microgravity*, pp. 21–45, 2001.

[31] C. V. N. Abbe, "Contribution à la modélisation 0D de la combustion Diesel: Application au Biodiesel," PhD Thesis, 2016.

[32] M. S. Kharasch, *Heats of combustion of organic compounds*. US Government Printing Office, 1929.

[33] J. C. O. Santos, J. P. Dantas, A. G. de Souza, and M. M. da Conceição, "Specific heat of Some vegetable oils by differential scanning calorimetry and microwave oven," in *II Congresso Braileiro de Plantas Oleaginosas, Oleos, Gorduras e Biodiesel Realizacao*, 2002, pp. 610–614.

[34] J. Serrano, F. J. Jiménez-Espadafor, A. Lora, L. Modesto-López, A. Gañán-Calvo, and J. López-Serrano, "Experimental analysis of NOx reduction through water addition and comparison with exhaust gas recycling," *Energy*, vol. 168, pp. 737–752, 2019.

[35] O. Grondin, "Modélisation du moteur à allumage par compression dans la perspective du contrôle et du diagnostic," PhD Thesis, Rouen, 2004.

[36] P. Sekmen and Z. Yılbaşı, "Application of energy and exergy analyses to a CI engine using biodiesel fuel," *Mathematical and Computational Applications*, vol. 16, no. 4, pp. 797–808, 2011.